

Improving strain diagnosis of prion disease by diffusion MRI and biophysical modelling

Marco Palombo³, Matteo Figini³, Riccardo Pascuzzo¹, Paola Caroppo², Mattia Verri¹, Torben Schneider⁴, Claudia A. M. Gandini Wheeler-Kingshott⁵, Veronica Redaelli², Daniel Alexander³, Hui Zhang³, Giorgio Giaccone², Alberto Bizzi¹

1 Neuroradiology, Fondazione IRCCS Istituto Neurologico “Carlo Besta”, Milano, Italy

2 Neurology, Fondazione IRCCS Istituto Neurologico “Carlo Besta”, Milano, Italy

3 Centre for Medical Image Computing, Department of Computer Science, University College London, London, UK

4 Philips United Kingdom, Guildford, Surrey, United Kingdom

5 Queen Square MS Centre, UCL Institute of Neurology, Faculty of Brain Sciences, University College London, London, United Kingdom

Synopsis

Sporadic Creutzfeldt–Jakob disease (sCJD) is the most common form of prion disease, characterized by five different strains, presenting intracellular vacuoles with different diameter/distribution. Unfortunately, no reliable non-invasive method for strain identification currently exists.

Here we provide the first quantitative maps of MR-measured vacuolar diameter/density in five sCJD patients, using multishell diffusion MRI and biophysical modelling. Results show distribution of small and larger vacuoles in the brain lesions of each patient, presumably corresponding to different sCJD strains, and absence of vacuoles in five age-matched healthy controls. If validated, this method would be extremely valuable for non-invasive diagnosis of sCJD strain.

INTRODUCTION

The purpose of this study is to improve the strain diagnosis in prion disease by estimating the distribution of vacuoles size from DW-MRI in the brain of Sporadic Creutzfeldt–Jakob disease (sCJD) patients.

sCJD is the most common human form of prion disease, a rare, transmissible, rapidly progressive and fatal neurological disease¹. sCJD is a heterogeneous disease with five different strains, having different lesion distribution, prognosis and requiring different treatment. Fine spongiosis is characteristic of the most common sCJD forms (MM1 and MV1), having a survival time of few months, while others (MM2 and MV2C) have large confluent vacuoles^{2,3} and longer survival time. One fifth of the patients may host more than one strain at the time. Unfortunately, no reliable non-invasive method for strain identification is currently available.

Diffusion MRI (DW-MRI) identifies sCJD lesions in the cortex, striatum and thalami with a diagnostic accuracy greater than 90%⁴. The neuropathological basis of DW-MRI hyperintensities is unknown, but a few studies suggested that the main determinant may be spongiform degeneration: the formation of intracellular vacuoles in brain tissues⁵⁻⁸. *In vivo*, non-invasive strain diagnosis will become very important once a treatment will be found.

METHODS

DW-MRI images from five patients with probable sCJD and five age-matched healthy controls were acquired on a 3T MRI scanner (Philips Achieva) using a Pulsed-Gradients-Stimulated-Echo (STEAM) sequence with parameters summarized in **Tab.1**.

All the data were denoised using MP-PCA⁹, Gibbs ringing¹⁰, eddy-current and motion artifacts corrected using FSL¹¹. The signal in each b shell was normalized by the corresponding b=0 and averaged across directions to compute the direction-averaged normalized signal S as a function of b. A tissue-inspired three compartment model, developed starting from previous work⁸:

$$S(b)/S(b=0) = f_{sticks} S_{sticks}(b, D_a) + f_{sphere} S_{sphere}(b, D_0=3 \mu\text{m}^2/\text{ms}, d_{sphere}) + (1 - f_{sticks} - f_{sphere})S(b, D_{iso})$$

was fitted to measured S(b) to estimate f_{sticks} (measure of neurites MR signal fraction), axial diffusivity D_a , f_{sphere} (measure of vacuoles MR signal fraction), d_{sphere} (MR measure of vacuoles diameter) and extra-cellular isotropic diffusivity D_{iso} . Note that the data were acquired at long diffusion time ($\Delta\delta/3=67$ ms) in order to minimise the possible confounding signal from cell bodies^{12,13}, and that the MR signal fractions are T_1 - T_2 weighted estimates.

Bilateral regions of interest (ROIs) were manually drawn in eleven regions: precuneus, parietal, frontal, temporal, occipital and anterior cingulate cortex, insula, hippocampus, caudate, putamen, dorso-medial thalamus. Thresholds on fractional anisotropy ($FA < 0.3$) and mean diffusivity ($MD < 2 \times 10^{-3} \text{mm}^2/\text{s}$) were used to exclude partial volume from white matter and CSF.

The distribution of vacuole diameters, weighted according to the fraction of the spherical compartment, was evaluated in the hyperintense part of each ROI.

RESULTS

DW-MRI showed the typical hyperintensities in all five sCJD patients, with variable involvement of the cortical areas and striatum (**Fig.1**).

The maps of the volumetric MR signal fraction of the spherical restricted compartment show values up to 0.35 in sCJD, with focal areas of high density, largely corresponding to hyperintensities on DW-MRI while they are uniform and generally below 0.15 in controls (**Fig.2**, right). The MR measured diameter size of the spheres (vacuoles) in the restricted compartment was in the range between 4-18 μm , in agreement with histological values reported in literature¹⁴ (**Fig. 2**, left). Vacuolar size distribution varied among patients: larger diameters were found in patient #1 and #4, with a peak around 13 and 15 μm respectively; small diameters were found in the striatum of patient #2; a bimodal distribution was estimated in patient #3, with a prevalence of smaller and larger vacuoles respectively; a broader distribution of diameters was found in #5 (**Fig.3**, left). The contribution of each anatomic region to these distributions is shown in the right columns of **Fig.3**.

So far, autopsy brains were collected in patients #2 and #3 and eventually more brains will be collected as patients will pass away. Point to point correlation with histopathology results is in progress and will be presented at the ISMRM meeting.

DISCUSSION and CONCLUSION

We showed the feasibility of generating quantitative maps of MR-measured vacuolar size and density in the brain of sCJD patients. The range of vacuolar sizes measured is compatible with histopathology results¹⁴. We found different distribution in patient with presumably different sCJD strains. In this small group of patients, larger diameters were estimated in the cortex than in the striatum.

If these results will be validated by neuropathology and confirmed in a larger group of patients, this method will become extremely valuable for the non-invasive diagnosis of sCJD strain, with an impact on more accurate prognosis and personalised therapy.

ACKNOWLEDGMENTS

This work was supported by the European Union's Horizon 2020 research and innovation programme under grant agreement nr. 666992 and by EPSRC (EP/G007748, EP/I027084/01, EP/L022680/1, EP/M020533/1, N018702, EP/M507970/1)

REFERENCES

- 1 Gambetti P., et al. *Br. Med. Bull.* 2003, 66, 213-239
- 2 Parchi P., et al. *Acta Neuropathol.* 2012, 124 (4), 517-529
- 3 Iwasaki Y. Creutzfeldt-Jakob disease. *Neuropathology* 2017, 37, 174–188
- 4 Puoti, G., et al., *The Lancet Neurology* 2012, 11(7), 618-628.
- 5 Geschwind M.D., et al. *Alzheimer Dis. Assoc. Disord.* 2009, 23 (1), 82-87.
- 6 Manners D.N., et al. *Neurology* 2009, 72 (16), 1425-1431
- 7 Lodi R., et al. *Brain* 2009, 132 (10), 2669-2679
- 8 Figini, M., et al. *Neuroimage: Clinical* 2015, 7, 142-154.
- 9 Veraart, J., et al. *Neuroimage* 2016, 142, 394-406.
- 10 Kellner, E., Dhital, B., Kiselev, V. G., Reiser, M. *M.R.M.* 2016, 76(5), 1574-1581.
- 11 <https://fsl.fmrib.ox.ac.uk/fsl>
- 12 Palombo, et al., *Proc. Int. Soc. Magn. Reson. Med.* 2018, #0892.
- 13 Palombo, et al., *Proc. Int. Soc. Magn. Reson. Med.* 2018, #1096.
- 14 Kovacs GG, Budka H, *Am J Pathol.* 2008, 172(3) :555-65

Tab.1 Protocol parameters to acquire the DW-MRI datasets using a Pulsed-Gradients-Stimulated-Echo (STEAM) sequence.

	TE (s)	δ (s)	Δ (s)	G (T/m)	b (s/mm ²)	# G directions	Time (sec)	TR (ms)	thickness (mm)	# slices	gap (mm)	coverage (mm)	FOV	matrix	nominal resolution
Shell1	0,070	0,025	0,075	0,018	1000	9	36	2754	2	15	4	90	256x256	128x126	2x2x2
Shell2	0,070	0,025	0,075	0,026	2000	9	36	2754	2	15	4	90	256x256	128x126	2x2x2
Shell3	0,070	0,025	0,075	0,032	3000	24	74	2754	2	15	4	90	256x256	128x126	2x2x2
Shell4	0,070	0,025	0,075	0,037	4000	24	74	2754	2	15	4	90	256x256	128x126	2x2x2
Shell5	0,070	0,025	0,075	0,041	5000	36	118	2754	2	15	4	90	256x256	128x126	2x2x2
Shell6	0,070	0,025	0,075	0,045	6000	36	118	2754	2	15	4	90	256x256	128x126	2x2x2
Shell7	0,070	0,025	0,075	0,052	8000	36	118	2754	2	15	4	90	256x256	128x126	2x2x2

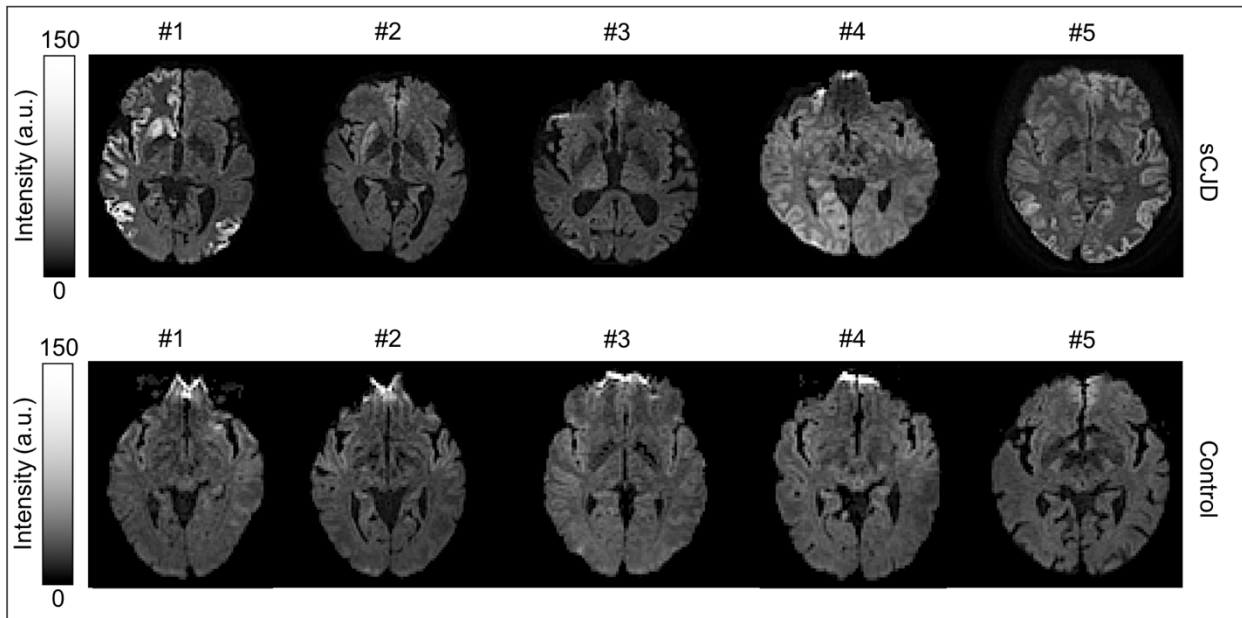


Fig.1 Representative dMRI slices acquired at $b = 1000 \text{ s/mm}^2$ for the five sCJD patients (top) and the five healthy controls (bottom). The patients images show the typical hyperintensities of CJD in the cortex and basal ganglia

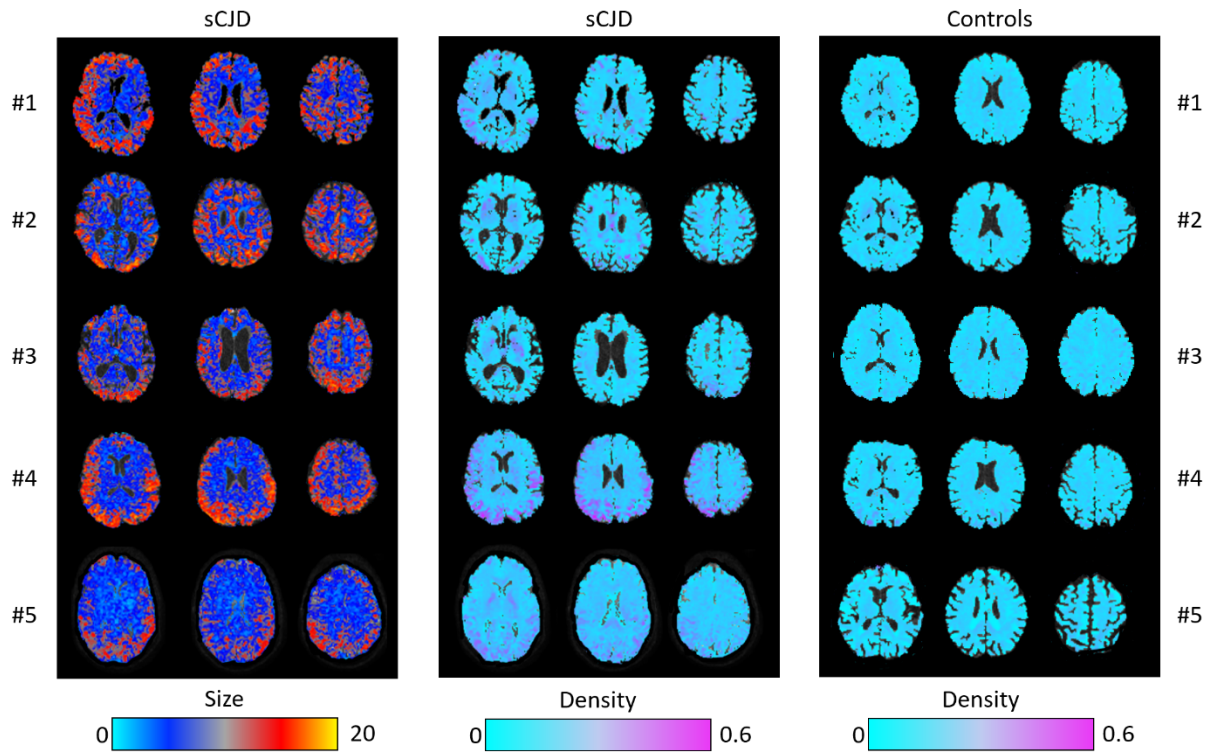
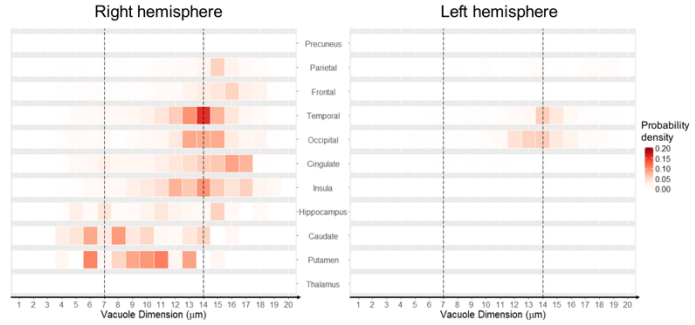
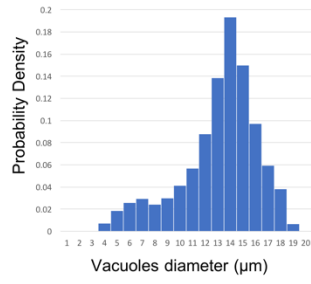
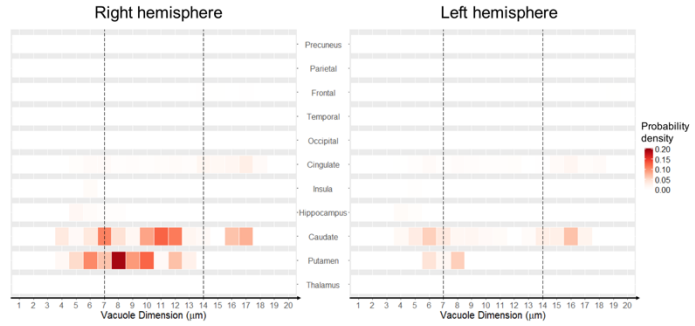
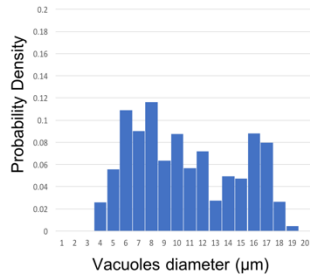


Fig.2 *Left:* Maps of MR measured diameter in μm (left) in each sCJD patient. *Middle:* MR signal fraction of the spherically restricted compartment (vacuole density) in each sCJD patient. In sCJD higher density values are found in brain regions with hyperintensities on DW-MRI (**Fig. 1**). *Right:* for comparison, MR signal fraction of the spherically restricted compartment in each healthy control. Values are always lower than 0.15.

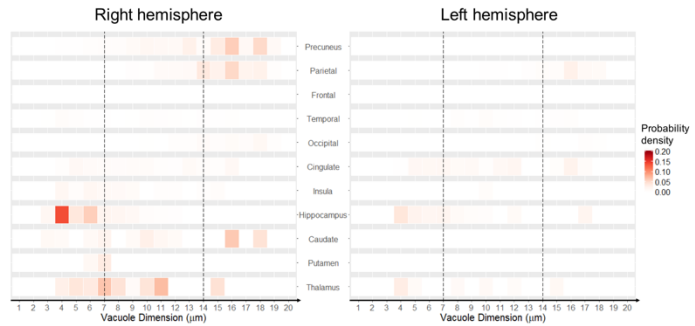
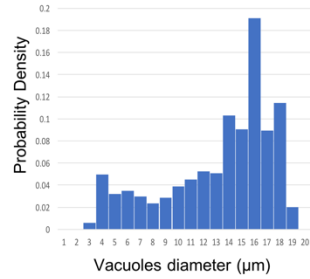
sCJD #1



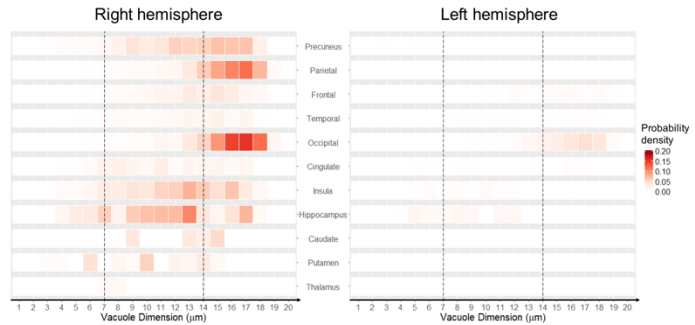
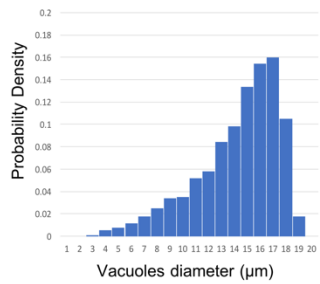
sCJD #2



sCJD #3



sCJD #4



sCJD #5

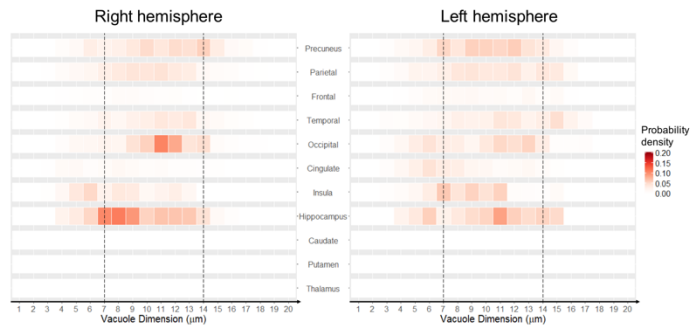
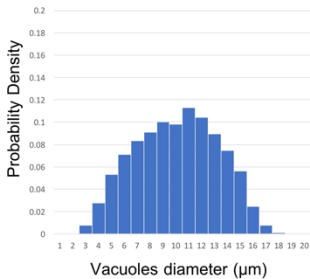


Fig.3 *Left column:* probability density distributions of MR measured vacuole size (in μm) in the hyperintense area of each brain, weighted by MR measured vacuole density. *Right columns:* probability density distribution of MR measured vacuole size (in μm) in each ROI, weighted by MR measured vacuole density.